Velocity distributions in vertically vibrated granular media

J. Delour[1,*], A. Kudrolli[1,2], and J.P. Gollub[1,3]
[1]*Department of Physics, Haverford College, Haverford PA 19041, U.S.A.*
[2]*Department of Physics, Clark University, Worcester MA 01610, U.S.A.*
[3]*Physics Department, University of Pennsylvania, Philadelphia PA 19104, U.S.A*

(December 2, 2024)

Abstract

We present an experimental, numerical and theoretical study of the probability distributions $P(v_i)$ of particle velocity components for a partial layer of inelastic colliding beads driven by a vertically oscillating boundary. Experimentally, we show that over a wide range of parameters (accelerations 3-8 times the gravitational acceleration), $P(v_i)$ is nearly Gaussian for the two horizontal components. A numerical simulation shows similar behavior, and indicates that the distribution of the vertical velocity v_z is also Gaussian. The sharing of the energy among the three velocity components is studied both numerically and theoretically. We find that the variances $T_i =< v_i^2 >$ of $P(v_i)$ are unequal, as one might expect given the asymmetry of the driving: $T_x = T_y$ but $T_z > T_x$, where x, z correspond to the horizontal and vertical components. The anisotropy increases as the particles are made more inelastic. Approximate analytical expressions are derived for the variances T_x and T_z as functions of the vibration amplitude and inelasticity. These predictions are consistent with the experimental measurements and simulations. Finally, we experimentally examine the sharing of energy between particles of different mass. The more massive particles are found to have greater kinetic energy, but the difference declines as the fractional coverage of the layer increases.

PACS: 83.70.Fn, 05.20.Dd, 46.10.+z, 83.10.Pp

*current address : Ecole Normale Superieure, 45 rue d'Ulm, 75005 Paris, France

I. INTRODUCTION AND BACKGROUND

Vibrated granular media have played a special role in efforts to understand the dynamics of granular materials [1,2], in part because it is a convenient method of replacing the energy lost to friction and inelasticity. A variety of novel phenomena have been discovered in the past fifteen years [3]: heaping and convection rolls [4,5], standing and traveling waves [6–8], and fluidization [9–11].

In treating strongly excited granular media, assumptions similar to those in kinetic theory are often made in order to derive a statistical theory for granular materials. Among these assumptions are that velocity distributions are Gaussian and that the mean energy is shared equally among the various degrees of freedom. The principle of equipartition of energy is indeed a prerequisite for the applicability to granular materials of thermodynamic concepts such as "entropy" or "free energy" [12,13]. It is therefore important to establish the conditions under which these are good assumptions.

A number of studies on vibrated granular media have addressed these issues. Numerical simulations and theoretical derivations have shown that the presence of inelasticity in granular flows can lead to the formation of clusters, and as a consequence equipartition of energy fails [16–18]. Experiments performed in a horizontal two-dimensional layer were consistent with this predicted clustering effect [19]. Vertical one-dimensional experiments and simulations were performed earlier [10]; a crossover from a condensed (clustered) to a fluidized state was found as a function of the driving acceleration, the number of beads, and the coefficient of restitution. Deviations from equipartition due to clustering are straightforward to understand on physical grounds. Inelastic collisions imply a loss of energy each time a collision occurs. When particles begin to gather in a certain region of space, the rate of their collisions increases. The rate of energy loss for this group of clustered particles is thus greater, and the distribution of their velocities becomes narrower than that of the particles in less dense regions.

Clustering is not the only source of deviations from equipartition. For example, Knight and Woodcock [14] studied a model vibrationally excited granular system theoretically (without gravity) and concluded that equipartition need not be observed at high amplitude of excitation due to the anisotropy of the energy source. A two dimensional system (a vertical Hele Shaw cell) was studied experimentally by Warr, Huntley, and Jacques [20]. Velocity distributions, though approximately Gaussian, were checked and found to exhibit anisotropy between the vertical and horizontal motion: the horizontal velocity distribution was narrower than the vertical one. Grossman, Zhou, and Ben-Naim [15] considered a two-dimensional granular gas from a theoretical quasi-continuum point of view and found the density to be nonuniform and the velocity distributions to be asymmetric for "thermal" energy input from one side. McNamara and Luding [21] considered the sharing of energy between rotational and translational motion of the particles, and found violations of equipartition.

The scaling of the granular kinetic energy with vibration amplitude is also of interest in connection with the experiments to be discussed in the present paper. It has been considered experimentally by Warr et al. [20], numerically by Luding, Hermann, and Blumen [22], and

theoretically by Kumaran in the nearly elastic limit of weak dissipation [23]. The results of these different studies do not seem to be mutually consistent with each other, perhaps because different regimes were explored; the situation is unclear.

In this paper, we study the simple case of a single layer of particles with vertical excitation. We vary the fractional coverage of this layer and the amplitude of the driving waveform. We determine the degree to which the velocity distributions are Gaussian, an issue that previous experiments have left unresolved for granular particles that are free to move in three dimensions. In parallel numerical and analytical investigations, we also vary the coefficient of restitution ϵ of the particles. Our investigation is focussed on the shapes of the distributions of the velocity components, and the dependence of the variances of the distributions on these three parameters.

In Sec. II, we present the experimental setup. In Sec. III, we show that, in all the cases we treated experimentally, the velocity distribution $P(v_i)$ is close to Gaussian and the energy is shared equally between the two horizontal components v_x, v_y. We show precisely how the variance increases with driving amplitude and decreases with particle density. The energy sharing between particles of different types is also described here. To obtain information about the vertical velocity distribution, which is inaccessible experimentally, we present in Sec. IV a numerical simulation that takes gravity into account. It reproduces the observed behavior for v_x, v_y, and we show that over a wide range of parameters, $P(v_z)$ is also Gaussian, but with a different variance than that of the horizontal distribution. The relationship between the vertical and horizontal variances depends on the coefficient of restitution ϵ but not upon the vibration amplitude or the fractional coverage $\tilde{f} = f/f_c$, where f_c is the coverage for a compact crystal of beads. We find that the degree of anisotropy (i.e., the departure from equality of the vertical and horizontal variances) grows with the degree of inelasticity (decreasing ϵ). In Sec. V and Appendix A, we discuss the dependence of T_x and the degree of anisotropy on relevant parameters theoretically without using the equipartition assumption. The anisotropy is found to depend only on the coefficient of restitution of the collisions, and becomes quite pronounced as ϵ is reduced.

II. EXPERIMENTAL SETUP AND METHODS

The experiments are conducted in a circular container of diameter 32 cm made of delrin. It is driven vertically with sinusoidal acceleration at a single frequency [24]. The frequency used in the experiment is 100 Hz and the amplitude of the acceleration is in the range 3-8 g. The particles are typically glass beads 4 mm in diameter with fractional coverage $\tilde{f}$. Smaller beads 0.5 mm in diameter were also used. A glass cover prevents the beads from escaping from the container, but collisions with the cover are rare. When only one particle is present, we find that its horizontal velocity is constant. We conclude from this fact that the energy provided by the shaker contributes only to the vertical motion.

Our objective is to follow one particle among the others. This is accomplished by using a single white aluminum oxide particle among the glass beads. Its diameter is 4.8 mm and its mass is 2.6 times that of the glass beads. The normal coefficients of restitution between

aluminum oxide, glass, and delrin are estimated by measuring the height to which a particle bounces on a flat surface. They are: $\epsilon_{glass/glass} = 0.85$, $\epsilon_{AlOx/glass} = 0.71$, $\epsilon_{glass/delrin} = 0.92$ and $\epsilon_{AlOx/delrin} = 0.91$. These parameters are not very different from each other and we therefore expect qualitatively similar (but not identical) behavior for the aluminum oxide and glass beads. To check this assumption, we also did experiments using two samples of glass beads that differ only in color.

Images are taken at a resolution of 512×512 pixels using a Dalsa variable scan CCD camera controlled by the same computer that produces the driving waveform. The sampling interval corresponds to every fifth period (intervals of 0.1 s); images are always acquired at the same phase with respect to the forcing. The position of the white particle is detected to an accuracy of 1 pixel and is stored in real time. A typical 15 minute experiment contains 10,000 successive positions of the particle. The displacement between successive frames yields the particle velocity, averaged over 0.1 s. We project each step onto two perpendicular directions, denoted by x and y, and study the statistics of each one.

III. EXPERIMENTAL RESULTS

A sample trajectory of the tracked particle (10,000 samples) in a sea of 4 mm beads is shown in Fig. 1. Though edge effects are not apparent, we do not include points within 1.4 cm of the boundary in the analysis as a precaution. The corresponding x-velocity distribution is shown in Fig. 2, on both linear and logarithmic scales. Velocities are shown in units of the standard deviation σ. The distribution is consistent with a Gaussian out to 3.5 σ. A similar analysis for the y-velocity yields an essentially identical distribution with the same variance, as expected from the symmetry of the apparatus. The shape of the distribution was unchanged over the acceleration range 3 and 8 g. Similar results were also obtained when the sea of 4mm beads where replaced with multiple layers of smaller 0.5 mm beads.

In Appendix B, we discuss the effect on the measured distributions of the fact that approximately 3 collisions occur per sampling interval. The result obtained there is that the flatness F_V of the measured distribution is related to the flatness F_v of the instantaneous velocity distribution by the formula $F_V = 2 + F_v/3$. The flatness is a useful statistic to describe the deviation from a Gaussian, for which $F = 3$. We are thus able to link the flatness of the measured distribution and that of the instantaneous velocity. The typical measured distribution (see Fig.2) has a flatness $F_V = 3.4$ when we include the data up to 3.5 σ. That would imply that the flatness for the instantaneous velocity distribution could be as large as $F_v = 4.2$. Thus, it may be concluded that $P(v_i)$ is also reasonably close to a Gaussian, though there could be small deviations.

We carefully varied the fractional coverage over the range 14% to 97%. The measured distribution is always consistent with a Gaussian, except when the fractional covering is high (near 97%) and the acceleration is lower (3-5 g). In that case, the layer is predominantly a crystalline lattice with defects. Particles jump out of the lattice occasionally and wander over it, eventually filling a vacancy elsewhere. It was difficult to collect sufficient data in

this case, since jumps by the tracer particle (or any individual particle) were rare. However, the velocity distribution clearly would have a large peak near zero in this case.

In the Gaussian regime, the variance T_i of the velocity distribution $P(v_i)$ is of course proportional to the kinetic energy of the motion in the direction i. It is a function of the fractional coverage $\tilde{f}$, the amplitude of the acceleration A of the shaker, and the coefficient of restitution ϵ of collisions between particles. The behavior of the variance as a function of A for different coverages $\tilde{f}$ is plotted in Fig. 3. The variance increases with acceleration, and decreases with increasing coverage.

The measurements presented in Figs. 1-3 were performed by tracking a (more massive) aluminum oxide particle in a background of glass spheres. To ensure that the mass difference did not affect our conclusions, we later repeated some of the measurements using glass particles differing only in color. Our conclusions about the velocity statistics were the same in this case. In addition, we were able to determine the energy sharing between particles of differing mass. We show in Fig. 4 the energy ratio of the aluminum oxide and glass particles when both were present, for several different accelerations. The more massive aluminum oxide particles have more kinetic energy. We note that the energy ratio is apparently not significantly dependent on the acceleration. As the coverage increases, however, the difference declines. Therefore, one can imagine that granular particles of different mass might share energy equally (as would perhaps be anticipated by analogy with the zeroth law of thermodynamics) when the coverage is so high that the particles interact much more frequently with each other than with the vibrator.

IV. SIMULATION

Here we report a numerical simulation that is intended to be appropriate to our experimental configuration. We describe our method and give the main differences relative to the simulation reported by Knight and Woodcock [14], which yields rather different results. The simulation is three-dimensional and is event-driven. We include gravity in our model and do not constrain the height, whereas Knight and Woodcock do not include gravity and use two moving walls in order to confine the particles. Our simulation is for coverages less than one full layer. Collisions are treated with the simplest possible model: when two particle collide, we multiply the normal velocities (in the center-of-mass frame of reference) by a factor $-\epsilon$ and leave the tangential velocities unchanged. We realize that a more realistic model is Walton's, which involves three coefficients of restitution and friction (one for the normal component of the velocity and two for the tangential component); this model has been tested experimentally by Lorentz, Tuozzolo and Louge [25]. However, we chose to consider only the normal coefficient of restitution in our simulation for the sake of simplicity: the inclusion of tangential coefficients would require the computation of angular momentum.

Collisions with the driver have been simplified in the simulation. In order to avoid the multiple collisions which can occur when a particle reaches the bottom plate [20], we require that the wall's vibration amplitude be small compared to the size of the particles and the mean distance between them. We fix the position of the plate, reverse the velocity of the

incident particle at the collision, and add a velocity increment $\overline{v_s}\{1+cos(\omega t)\}$ where t is the time of the collision. We checked that the results do not depend significantly on the precise method used to simulate boundary collisions. (For example, using a time-independent velocity increment, or varying the frequency leads to essentially the same results.)

The simulations produce data similar to that of the experiment. They also provide access to the vertical motion, which is inaccessible in our experimental geometry. We compute 10,000 samples of the instantaneous velocity, in this case without averaging, and determine statistical distributions of v_x, v_y and v_z. They turn out to be Gaussian with very good precision.

We also compute, as we did for the experiment, the variances T_x, T_y and T_z of these distributions for various coverages and driving accelerations. In this case we use a sampling interval of 0.1 s for comparability with the experiments of Fig. 3. (This has the effect of reducing the computed variances by a factor equal to the mean number of collisions in that time.) When the density is fixed, we obtain the behavior shown in Fig. 5. The variances increase with acceleration as in the experiment; the x and y values are equal and close to those found experimentally, and there is greater energy in the z direction. For a given acceleration, T_x decreases when the density increases as in the experiment.

The simulation indicates that the kinetic energy can be distributed unequally among the three translational degrees of freedom while remaining Gaussian. Warr *et al.* [20] observed this phenomenon in their two-dimensional vertical channel experiment with many layers, but considered the effect negligible and used the assumption of equipartition in their derivations.

We now discuss the sharing of the energy between the vertical and horizontal directions, as a function of $\tilde{f}$, A, and ϵ. When we fix $\tilde{f}$ and ϵ and vary A, we notice that the ratio $\tilde{T}_x = T_x/(T_x + T_y + T_z)$, which indicates the fractional energy in one horizontal component of the motion, and hence the degree of anisotropy, does not change. Knight and Woodcock also studied this ratio numerically, but did not find anisotropy (values of this ratio differing from 1/3) in our range of parameters, for which the amplitude of the shaking is much smaller than the characteristic distance between particles.

Having eliminated A as a relevant parameter, we show in Fig. 6, $\tilde{T}_x$ as a function of ϵ for various $\tilde{f}$. We notice that this ratio does not depend significantly on $\tilde{f}$ but does depend on the coefficient of restitution. For elastic collisions ($\epsilon = 1$) about 50% of the energy is in the vertical degree of freedom (and 25% in each of the horizontal ones). Increasing the inelasticity (reducing ϵ) augments the vertical/horizontal asymmetry.

It is not surprising that the energy sharing depends on the coefficient of restitution since all the energy provided to horizontal translation is provided by collisions between particles. We estimated numerically that a particle is involved in 2-5 particle collisions per boundary collision. However, it does seem surprising that $\tilde{T}_x$ is independent of the coverage and acceleration.

V. THEORY OF THE ANISOTROPY

We also have been able to treat the question of equipartition theoretically, to supplement the numerics of Sec. IV. We find from this calculation that in general the vertical and horizontal directions share energy differently, this division depending strongly and only on the coefficient of restitution. We are also able to derive the variances of the distributions with coverage and drive amplitude, and we compare these predictions with the experiments of Sec. III. We avoid the statistical assumption of equipartition of energy between vertical and horizontal motion.

Rather than presenting all the details in this section, we simply outline the method and present the results and figures; the full calculation, which is somewhat technical, is given in Appendix A. The basic idea is to take advantage of the fact gleaned from the numerics that the particle probability density varies exponentially with the z coordinate. Using this observation as an assumption, we are able to obtain an explicit expression for the probability for a binary collision at angle θ (relative to the vertical) to occur within a time interval dt. The calculation is two dimensional, but we are able to interpret the results in three dimensions, as explained shortly. The next step is to determine the energy lost in a θ-collision that is attributable to the horizontal coordinate. By requiring this energy loss to vanish on the average in the steady state, it is possible to obtain an expression relating the velocity variances T_x and T_z. The result for the fraction of the energy in the horizontal coordinate is given in Eq. (A12), which we reproduce here:

$$\frac{T_x}{T_x+T_z} = \frac{1}{1-\frac{2.48r^2-1.64r-0.65}{0.83(1-r)^2}} \quad , \tag{1}$$

where, $r = (1-\epsilon)/2$. To apply this result to the three-dimensional situation, we use the symmetry of the apparatus to infer that the energy must be shared equally between the two horizontal coordinates. This leads to the conclusion that in Eq. (1), T_x should be reduced by precisely a factor of two, T_y should be taken to be equal to T_x, and T_z should be left unchanged. The resulting values of $T_i/(T_x+T_y+T_z)$ for the x, y and z motions are shown in Fig. 7 as a function of ϵ over the interval $[0,1]$. This figure shows that the sharing of energy between vertical and horizontal coordinates becomes strongly anisotropic for small ϵ, a fact that is also immediately clear from the form of Eq. (1). This result is to be compared with the numerical simulation of Sec. IV (Fig. 6), which shows similar behavior.

Next, we consider the energy balance in the z direction, including the energy received from the shaker and from gravity. This process leads to an expression for T_x that can be approximated rather accurately as shown in Eq. (A21). We reproduce it here for convenience:

$$T_x = \frac{1}{6.5}\frac{L}{NR}\frac{\overline{v}_s^2}{(1-\epsilon)} \quad . \tag{2}$$

In this equation, L is the horizontal dimension of the system, L/NR is equivalent to the coverage $\tilde{f}$, and $\overline{v}_s$ is related to the acceleration amplitude A by $\overline{v}_s = A/\sqrt{2}\omega$. This is, with

a different numerical prefactor, the same as Eq. (24) of Warr, Huntley and Jacques [20]. We derived the result without assuming equipartition, but we do assume (as shown by the experiment) that the velocity distributions $P(v_i)$ are symmetric and we use a simple model of binary collisions.

This formula for the dependence of T_x on parameters is roughly consistent with the experimental results, as we show in Fig. 8 (compare with Fig. 3). To facilitate comparison with the expermental data, we divide the theoretical prediction by a factor of 2.5 corresponding to the mean number of collisions that occur during the experimental sampling interval, as explained in Appendix B. We find consistency with the experimental data to within about 20% over most of the range of observation. The theory is surely no better than that. However, the slopes at high acceleration in Fig. 8 seem somewhat larger than in the experiment (Fig. 3). This could be explained by the fact that the number of collisions between images probably increases somewhat with acceleration.

VI. SUMMARY AND CONCLUSION

We have reported experimental, numerical, and theoretical studies of velocity statistics for a (fractional) layer of glass beads subjected to vertical vibration. We find (by experiment and simulation) that in the steady state the distributions are nearly Gaussian (Fig. 2), though faster imaging would be needed for a more precise test. We also show experimentally that particles of different mass do not have the same kinetic energy when both are present simultaneously (Fig. 4), an apparent violation of equipartition. However, the difference declines with increasing coverage, and hence it is possible that the energies would be equal under circumstances where the particles interact much more frequently with each other than with the exciter.

We find (by simulation and theory) that the variances T_i of the velocity components v_i differ: $T_x = T_y$ and $T_z > T_x$. The ratio of the energy content in the vertical and horizontal degrees of freedom is shown to depend only on the coefficient of restitution for the collisions between particles (Figs. 6,7). The theory does not assume equipartition between vertical and horizontal degrees of freedom and in fact shows that there must be an asymmetry, a prediction that is consistent with our studies and the 2D experiments of Warr et al. [20]. The lack of equipartition between velocity components is due (at least primarily) to the inelasticity of particle collisions. Finally, we have experimentally determined the dependence of the variance T_x of a horizontal velocity component on coverage and on the acceleration amplitude experimentally (Fig. 3), and have derived a theoretical formula, Eq. (2) and Fig. 8, that is in reasonable accord with the experiments.

These studies and many others imply that thermodynamic concepts are not generally valid for these dissipative systems (though they may be useful in certain regimes), since violations of equipartition are clearly evident. The present work, in which the particles are free to move in three dimensions, extends previous investigations of the statistical properties of strongly excited granular particles. We find semiquantitative agreement between experiments, simulation, and theory where these methods overlap. It would be desirable to

study the vertical motion experimentally for comparison with Eq. (1), though our present instrumentatation does not allow this.

Acknowledgements: This work was supported in part by the National Science Foundation under Grants DMR-9319973 and DMR-9704301. Wolfgang Losert contributed substantially to experiments on the sharing of energy between particles of different mass. We are grateful to Yuhai Tu for a critical reading of the manuscript. Technical support was provided by Bruce Boyes.

APPENDIX A: DETAILS OF THE THEORETICAL CALCULATION

In this Appendix, we treat the question of equipartition theoretically, and we show that in general the vertical and horizontal directions share energy differently, this division depending strongly and only on the coefficient of restitution. We are also able to derive the variation of the distributions with coverage and drive amplitude, as studied in the experiments of Sec. III. We avoid the *a priori* statistical assumption of equipartion, and compare our results to previous calculations [20,14] where this assumption was made.

1. Probability for a θ-collision

We have seen in the experiment and numerically that the distribution $P(v_x)$ is the same as $P(v_y)$. Given this isotropy in the horizontal plane, one can derive the variance of the velocity distribution analytically using a two dimensional model. In two dimensions (x,z), a collision is completely characterized by the angle θ between the line joining the centers of mass of the two particles and the horizontal direction. In three dimensions, there is an additional azimuthal angle ϕ about the z axis. To recover the experimental or numerical results, one has to divide the horizontal energy found by the model equally between the x and y directions.

The simulations show that the probability to find the particle is uniform along x and nearly exponential along z : $p_z(z) = H^{-1}(\tilde{f}, A) exp[-z/H(\tilde{f}, A)]$, where $H(\tilde{f}, A)$ is the mean height of the bounces of a bead. Furthermore, the behavior of this average height is linear in the vertical temperature T_z : $H(\tilde{f}, A) = 2.66RT_z$, where R is the radius of a bead and 2.66 is the slope in s^2cm^{-2}.

The probability density for a particle to be in (x, z) with the precision (dx, dz) is therefore taken to be

$$p_{x,z}(x, z) = \frac{1}{H(\tilde{f}, A)L} e^{-\frac{z}{H(\tilde{f},A)}} \quad . \tag{A1}$$

where L is the horizontal dimension of the system. A similar probability density was also used in Ref. [23] and is consistent with a gaussian velocity distribution.

Let us consider an ensemble of similar systems at a time t with precision dt. The probability for one particle to be hit by another one is the probability for this particle to be at (x, z) while the other is at $(X = x + 2Rcos\theta, Z = z + 2Rsin\theta)$. It is $p_\theta(\theta) = p_{x,z}(x, z)p_{x,z}(X, Z)\ dx\ dz\ dX\ dZ$:

$$p_\theta(\theta) = \frac{1}{H(\tilde{f}, A)L} e^{-\frac{z}{H(\tilde{f},A)}}\ \frac{1}{H(\tilde{f}, A)L} e^{-\frac{z+2Rsin\theta}{H(\tilde{f},A)}}\ dx\ dz\ 2dR\ 2Rd\theta \quad , \tag{A2}$$

where $2dR\ 2Rd\theta$ is the Jacobian of the change of variables from (X, Z) to (R, θ), and dR is the tolerance with which R is specified. This function, integrated over the variables x and z, gives the probability for one particle to be involved in a collision at angle θ . We have to multiply by $N(N-1)/2$ to take into account all the possible combinations of binary collisions between the N particles.

We find that the probability for one θ-collision to occur at a time t with precision dt is given by

$$p_\theta(\theta) = 2\frac{N(N-1)}{H(\tilde{f}, A)L} e^{-\frac{2Rsin\theta}{H(\tilde{f},A)}} R\ dR\ d\theta \quad . \tag{A3}$$

In obtaining this expression, we are neglecting any dependence on the z coordinate, which has been integrated out. The adequacy of this approximation can only be tested by comparing the obtained in this section with simulations.

2. Energy lost in a θ-collision

When two particles collide, we take the normal and tangential projections of the velocities and proceed to analyze an inelastic collision in the laboratory (not the center of mass) frame of reference. If v_n and v_t are these projections, the collision is written

$$\begin{cases} v_n^{'i} = v_n^i(1-\epsilon)/2 + v_n^j(1+\epsilon)/2) \\ v_t' = v_t \end{cases} \quad . \tag{A4}$$

To obtain v_n and v_t from the measured v_x and v_z, we use a simple rotation matrix, treat the collision as described above, and return to the v_x and v_z coordinates. The kinetic energy gained or lost due to the momentum exchange in the x direction during a θ-collision is $\Delta E_x = (v_x^{'2\,i} + v_x^{'2\,j}) - (v_x^{2\,i} + v_x^{2\,j})$. If we define $r = (1-\epsilon)/2$, the expression found is:

$$\begin{aligned} \Delta E_x = {} & (A^2 + B^2 - 1)(v_x^{2\,i} + v_x^{2\,j}) + 2C^2(v_z^{2\,i} + v_z^{2\,j}) \\ & + 4ABv_x^i v_x^j - 4C^2 v_z^i v_z^j \\ & + 2(AC - BC)(v_x^i v_z^i + v_x^j v_z^j - v_x^j v_z^i - v_x^i v_z^j) \quad , \end{aligned} \tag{A5}$$

with

$$A = rcos^2\theta + sin^2\theta \quad , \quad B = (1-r)cos^2\theta \ \ and \ \ C = (1-r)cos\theta sin\theta \quad . \tag{A6}$$

3. Mean energy exchange resulting from the horizontal coordinate

We now compute the contribution to the kinetic energy exchange from motion along the x-direction: $\overline{\Delta E_x} =< (v_x'^{2\,i} + v_x'^{2\,j}) - (v_x^{2\,i} + v_x^{2\,j}) >$. By requiring this quantity to vanish in the steady state, it is possible to obtain an expression relating T_x and T_z.

We have found the probability of a θ-collision in Appendix A.1, and the variation of energy in a θ-collision in Appendix A.2. To proceed, we need the velocity distribution. The experiments presented in Sec. III show that it is always Gaussian over the range of the parameters we use. So we assume such a distribution with variances T_x, T_z corresponding to the x, z directions:

$$P(v_x) = \frac{1}{\sqrt{2\pi T_x}} e^{-\frac{v_x^2}{2T_x}} \quad and \quad P(v_z) = \frac{1}{\sqrt{2\pi T_z}} e^{-\frac{v_z^2}{2T_z}} \quad . \tag{A7}$$

We can now calculate $\overline{\Delta E_x}$ which is

$$\overline{\Delta E_x} = \int_{-\frac{\pi}{2}}^{\frac{\pi}{2}} p_\theta(\theta)\, d\theta \prod_{k=x,z}^{l=i,j} \left(\int_{-\infty}^{+\infty} dv_k^l \frac{1}{\sqrt{2\pi T_k}} e^{-\frac{v_k^{2\,l}}{2T_k}} \right) \Delta E_x \, dR \quad . \tag{A8}$$

Given the Gaussian probability for the velocities, it is only necessary to keep the squared velocities terms in ΔE_x; the others vanish. We just have to calculate A^2, B^2 and C^2; from Eqs. (5) and (6) we find

$$\begin{aligned} \Delta E_x = {} & (2cos^4\theta\, r^2 + 2cos^2\theta(sin^2\theta - cos^2\theta)\, r + sin^4\theta + cos^4\theta - 1)(v_x^{2\,i} + v_x^{2\,j}) \\ & + 2cos^2\theta sin^2\theta (1-r)^2 (v_z^{2\,i} + v_z^{2\,j}) \quad . \end{aligned} \tag{A9}$$

The Fubini theorem allows us to treat separately the integrals over θ, R and the velocities. The integrals over the velocities all have the form

$$\int_{-\infty}^{+\infty} v^2 \frac{1}{\sqrt{2\pi T}} e^{-\frac{v^2}{2T}}\, dv \; = T \quad . \tag{A10}$$

We use Eq. (A8) and work in the high temperature approximation where T_z is sufficiently large that the exponent in Eq. (A3) can be approximated by unity. This approximation is well satisfied by the experiments to be modeled. We find that

$$\overline{\Delta E_x} = 2\frac{N(N-1)}{2.66RT_zL} \{ T_x(2.48r^2 - 1.64r - 0.65) + 0.83\, T_z(1-r)^2 \} R\, dR \quad . \tag{A11}$$

Requiring $\overline{\Delta E_x} = 0$ in the steady state gives us a relationship between T_x and T_z. Expressing it as the fraction of the total energy corresponding to the x-motion, we find

$$\frac{T_x}{T_x + T_z} = \frac{1}{1 - \frac{2.48r^2 - 1.64r - 0.65}{0.83(1-r)^2}} \quad . \tag{A12}$$

We have discussed this prediction for the anisotropy in Sec. V and presented the results graphically in Fig. 7.

4. Mean energy balance in the z-direction

We can do a similar analysis for the z-direction. We have to include in the condition $\overline{\Delta E_z} = 0$ the energy received from the shaker and from gravity. We obtain for the collisional contribution to $\overline{\Delta E_z}$ the expression

$$\overline{\Delta E_z^{col}} = 2\frac{N(N-1)}{2.66\,R\,T_z\,L}\{0.83\,T_x(1-r)^2 + T_z(2.48\,r^2 - 1.64\,r - 0.65)\}R\,dR \quad . \tag{A13}$$

Let us now treat the contribution of gravity to this energy balance. The variation of the kinetic energy for one particle during the period dt at the time t is $\Delta E_z^{grav} = -mgv_z\ dt$. When we average over the positions and velocities of the particles we obtain a total contribution $\overline{\Delta E_z^{grav}} = 0$ because of the symmetric shape of the velocity distribution.

The shaker also contributes to the balance energy. We make the assumption that each collision occurs for $z = 0$ (*ie* the amplitude of oscillation of the shaker is small compared to the diameter of the particles), and the result of the collision is :

$$v_z^{'} = -v_z + v_s \quad , \tag{A14}$$

where $v_s = \sqrt{2}\ \overline{v}_s cos(\omega\,t)$. The variation of the kinetic energy for one collision with the bottom is

$$\Delta E_z^{bot} = v_z^{'\,2} - v_z^2 = -2\ v_z\sqrt{2}\ \overline{v}_s cos(\omega\,t) + 2\ \overline{v}_s^2 cos^2(\omega\,t) \quad . \tag{A15}$$

For a more detailed treatment of the exchange of energy with the shaker, see Ref. [20,14]. When we average over the position (anywhere where $z = 0$), the number of particles, the velocity distribution, and over a period of the shaking waveform, we obtain :

$$\overline{\Delta E_z^{bot}} = \frac{N}{2.66\,R\,T_z}\overline{v}_s^2\,dz \quad . \tag{A16}$$

The balance equation is then $\overline{\Delta E_z^{col}} + \overline{\Delta E_z^{bot}} = 0$, that is to say

$$2\frac{N(N-1)}{2.66\,R\,T_z\,L}\{0.83\,T_x(1-r)^2 + T_z(2.48\,r^2 - 1.64\,r - 0.65)\}R\,dR = -\frac{N}{2.66\,R\,T_z}\overline{v}_s^2\,dz \quad . \tag{A17}$$

Now $dR \simeq dz \simeq \overline{v}\ dt$ where $\overline{v}$ is the typical velocity of the particles and $N - 1 \simeq N$ since the number of particles is large. We obtain

$$2\frac{NR}{L}\{0.83\,T_x(1-r)^2 + T_z(2.48\,r^2 - 1.64\,r - 0.65)\} = -\overline{v}_s^2 \quad . \tag{A18}$$

5. Dependence of the variance T_x on inelasticity:

We have obtained two independent balance equation involving T_x and T_z. We can introduce the first one into the second one to obtain an expression for T_x :

$$T_x = -\frac{1}{f(r)}\frac{L}{NR}\overline{v}_s^2 \quad , \tag{A19}$$

where $f(r)$ is the following function :

$$f(r) = 2\{\ 0.83(1-r)^2 - \frac{(2.48\,r^2 - 1.64\,r - 0.65)^2}{0.83(1-r)^2}\ \} \quad . \tag{A20}$$

When we plot $f(r)$, we find it to be very close to $-13(1-\epsilon)$, where $\epsilon = 1-2r$. The final prediction for T_x is

$$T_x = \frac{1}{6.5}\frac{L}{NR}\frac{\overline{v}_s^2}{(1-\epsilon)} \quad . \tag{A21}$$

We have discussed this equation (and Fig. 8 which was obtained from it) in Sec. V.

APPENDIX B: MEASURED VERSUS INSTANTANEOUS VELOCITY DISTRIBUTION

In this Appendix, we discuss the effect of the finite sampling interval on the measured velocity distributions. We show that the velocity distribution measured in the experiment has a smaller variance by a factor equal to the mean number $\bar{n}$ of collisions in the sampling interval, and the flatness of the distribution is also affected. On the other hand, if $\bar{n}$ is fairly small, departures from Gaussian behavior can still be detected detected with good accuracy. By simulation, we find $\bar{n} \approx 2.5$ in our experiments.

For simplicity, we suppose $\bar{n}$=3 in this Appendix, so the measured velocity is assumed to be averaged over 3 collisions separated by equal time intervals. Let us denote this average velocity by V and the instantaneous velocity by v. Letting $\Phi(k)$ be the characteristic function of the distribution of $P(V)$, we have

$$\Phi(k) = \int_{-\infty}^{\infty} dV\ e^{ikV} P(V) = \sum_{n=0}^{\infty} \frac{(ik)^n < V^n >}{n!} \quad .$$

The limited expansion of $\Phi(k)$ gives the moments of the distribution. Let us denote by $\phi(k)$ the characteristic function of the instantaneous distribution $p(v)$. A classical result gives

$$\Phi(k) = \phi^3(\frac{k}{3}) \quad .$$

We thus can find a relationship between the moments of $P(V)$ and the ones of $p(v)$. Our distributions are even and have null odd moments. The relationships between the second and fourth moments for the two distributions are

$$< V^2 >= \frac{< v^2 >}{3} \quad ;$$

$$< V^4 >= \frac{2}{9} < v^4 > + \frac{1}{27} < v^2 >^2 \quad .$$

The flatness of a distribution $f(x)$ is defined by

$$F_x = \frac{< x^4 >}{< x^2 >^2} \quad .$$

Its value is 3 for a Gaussian distribution and can be used as a parameter to determine the deviations from Gaussian behavior. In our case, for 3 collisions, we have

$$F_V = 2 + \frac{1}{3} F_v \quad .$$

This result is used in Sec. III.

REFERENCES

[1] C.S. Campbell, *Annu. Rev. Fluid Mech.* **22**, 57 (1990).
[2] H.M. Jaeger, S.R. Nagel and R.P. Behringer, *Phys. Today* **49**, No. 4, 32 (1996).
[3] P. Evesque, *Contemp. Phys.* **33**, 245 (1992).
[4] P. Evesque and J. Rajchenbach, *Phys. Rev. Lett.* **62**, 44 (1989).
[5] E.E. Ehrichs, H.M. Jaeger, G.S. Karczmar, J.B. Knight, Vadim Yu. Kuperman and S.R. Nagel, *Science* **267**, 1632 (1995).
[6] S. Douady, S. Fauve and C. Laroche, *Europhys. Lett.* **8**, 621 (1989).
[7] H.K. Pak and R.P. Behringer, *Phys. Rev. Lett.* **71**, 1832 (1993).
[8] F. Melo, P.B. Umbanhowar and H.L. Swinney, *Phys. Rev. Lett.* **75**, 3838 (1995).
[9] E. Clément, S. Luding, A. Blumen, J. Rajchenbach and J. Duran, *Int. J. Mod. Phys.* B **7**, 1807 (1993).
[10] S. Luding, E. Clément, A. Blumen, J. Rajchenbach and J. Duran, *Phys. Rev. E* **49**, 1634 (1994).
[11] E. Clément and J. Rajchenbach, *Europhys. Lett.* **16**, 133 (1991).
[12] S.F. Edwards, *J. Stat. Phys.* **62**, 889 (1991).
[13] H.J. Herrmann, *J. Phys. II France* **3**, 427 (1993).
[14] T.A. Knight and L.V. Woodcock, *J. Phys. A* **29**, 4365 (1996).
[15] E.L. Grossman, T. Zhou and E. Ben-Naim, *Phys. Rev. E* **55** , 4200 (1997).
[16] M.A. Hopkins and M.Y. Louge, *Phys. Fluids A* **3**, 47 (1991).
[17] I. Goldhirsch and G. Zanetti, *Phys. Rev. Lett.* **70**, 1619 (1993).
[18] Y. Du, H. Li and L.P. Kadanoff, *Phys. Rev. Lett.* **74**, 1268 (1995).
[19] A. Kudrolli, M. Wolpert and J.P. Gollub, *Phys. Rev. Lett.* **78**, 1383 (1997).
[20] S. Warr, J.M. Huntley and G.T.H. Jacques, *Phys. Rev. E* **52**, 5583 (1995).
[21] S. McNamara and S. Luding, preprint cond-mat/9805257 (1998).
[22] S. Luding, H.J. Hermann and A. Blumen, *Phys. Rev. E* **50**, 3100 (1994).
[23] V. Kumaran, *Phys. Rev. E* **57**, 5660 (1998).
[24] A. Kudrolli and J.P. Gollub, *Physica D* **97**, 133 (1996).
[25] A. Lorentz, C. Tuozzolo and M.Y. Louge, *Experimental Mechanics* **37**, 292 (1997).

FIGURES

FIG. 1. Measured trajectory of a white particle moving among a layer of dark ones. The container is vertically shaken at 100 Hz and acceleration 4 g. Ten thousand sequential position measurements are acquired at a frequency of 10 Hz.

FIG. 2. Velocity distribution of the tracked particle plotted on linear (a) and logarithmic (b) scale in units of the standard deviation $\sigma = 3.94$ cm/s (driving acceleration $A = 5$ g, coverage $\tilde{f} = 0.42$). The Gaussian fit is a good approximation up to 3.5 σ.

FIG. 3. Measured variance T_x of the velocity distribution $P(v_x)$ for 5 fractional coverages as a function of the driving acceleration amplitude A. The variance increases with A and decreases with $\tilde{f}$. The lines are drawn to guide the eye.

FIG. 4. Measured ratio of kinetic energies of aluminum oxide and glass particles as a function of coverage. There is no significant dependence on acceleration. The more massive aluminum oxide particles have greater energy, but the ratio declines as the frequency of interparticle collisions increases.

FIG. 5. Variances T_x, T_y, and T_z in the *numerical simulation* as a function of the driving acceleration amplitude A, for 38% coverage and coefficient of restitution $\epsilon = 0.9$. We have used a sampling interval of 0.1 s in the simulations for comparability with the experiments of Fig. 3. Note that $T_x = T_y$ but $T_z > T_x$.

FIG. 6. Fractional kinetic energy corresponding to x, y and z-motions in the *numerical simulation*, for several fractional coverages, as a function of the coefficient of restitution ϵ. Inelasticity augments the anisotropy, but these ratios are independent of coverage.

FIG. 7. Fractional kinetic energy corresponding to x, y and z-motions in the *theoretical* prediction of Eq. (1), for several fractional coverages, as a function of the coefficient of restitution ϵ. The behavior is similar to that of the simulation in Fig. 6.

FIG. 8. Theoretical variance T_x of $P(v_x)$ for 4 fractional coverages as a function of acceleration A. It has been reduced by a factor of 2.5 equal to the mean number of collisions in the experimental sampling interval for comparison with the data of Fig.3.

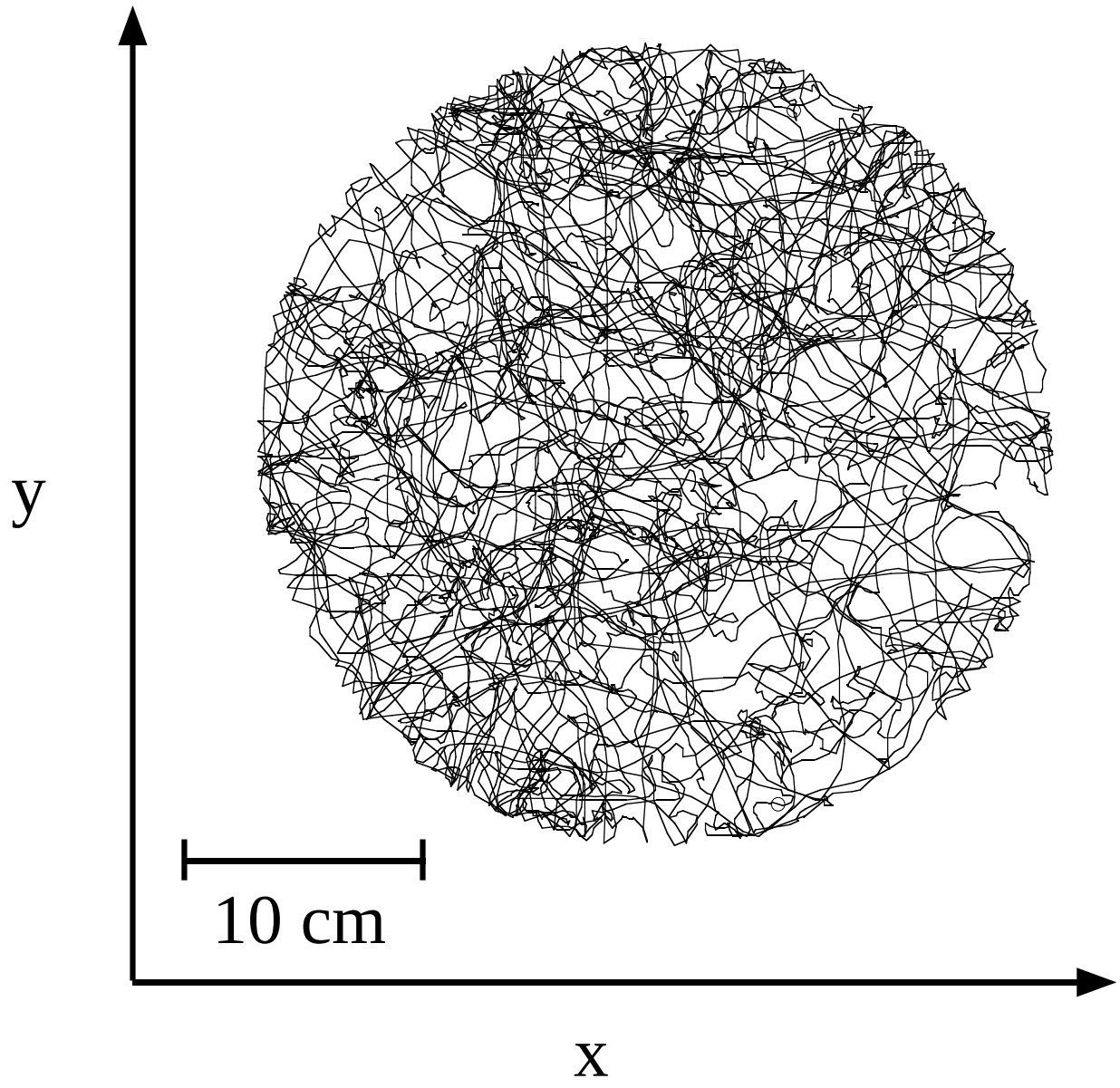

FIG. 1. Measured trajectory of a white particle moving among a layer of dark ones. The container is vertically shaken at 100 Hz and acceleration 4 g. Ten thousand sequential position measurements are acquired at a frequency of 10 Hz.

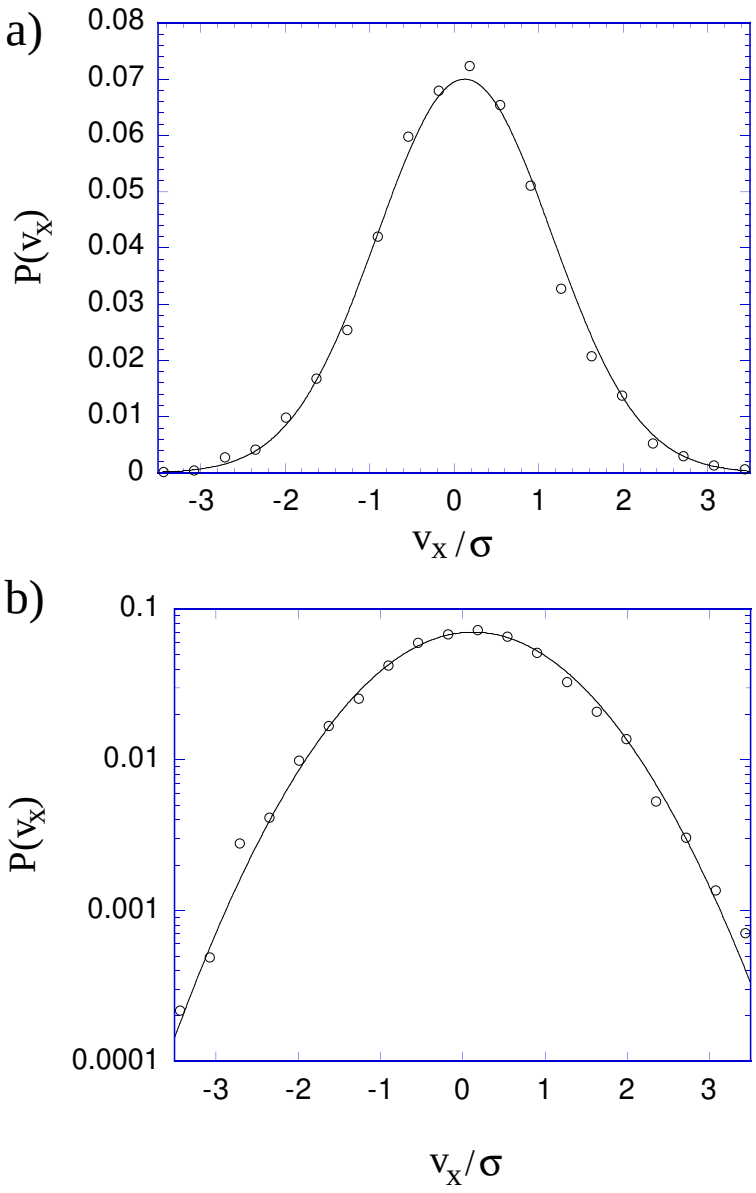

FIG. 2. Velocity distribution of the tracked particle plotted on linear (a) and logarithmic (b) scale in units of the standard deviation $\sigma = 3.94$ cm/s (driving acceleration $A = 5$ g, coverage $\tilde{f} = 0.42$). The Gaussian fit is a good approximation up to 3.5 σ.

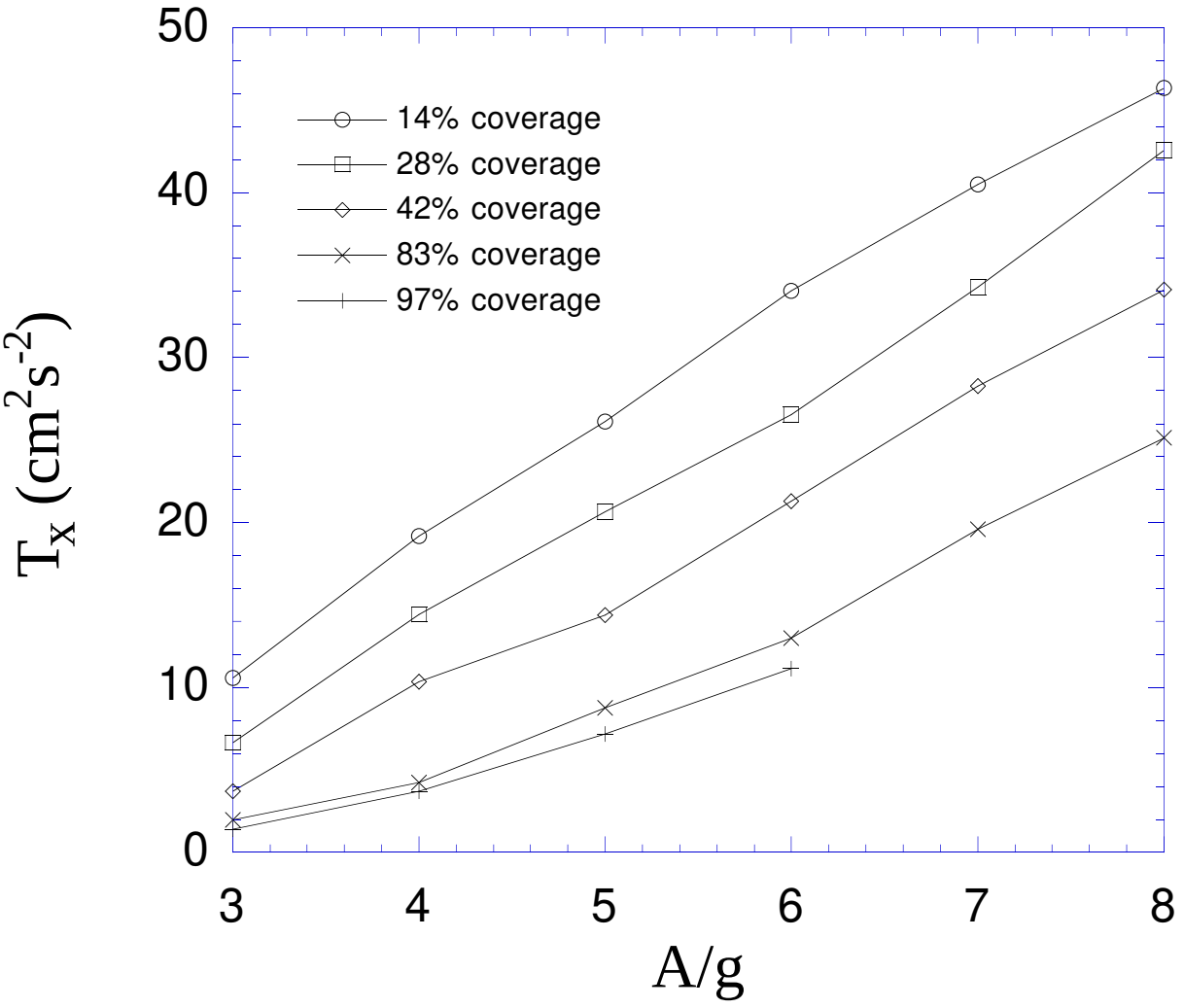

FIG. 3. Measured variance T_x of the velocity distribution $P(v_x)$ for 5 fractional coverages as a function of the driving acceleration amplitude A. The variance increases with A and decreases with $\tilde{f}$. The lines are drawn to guide the eye.

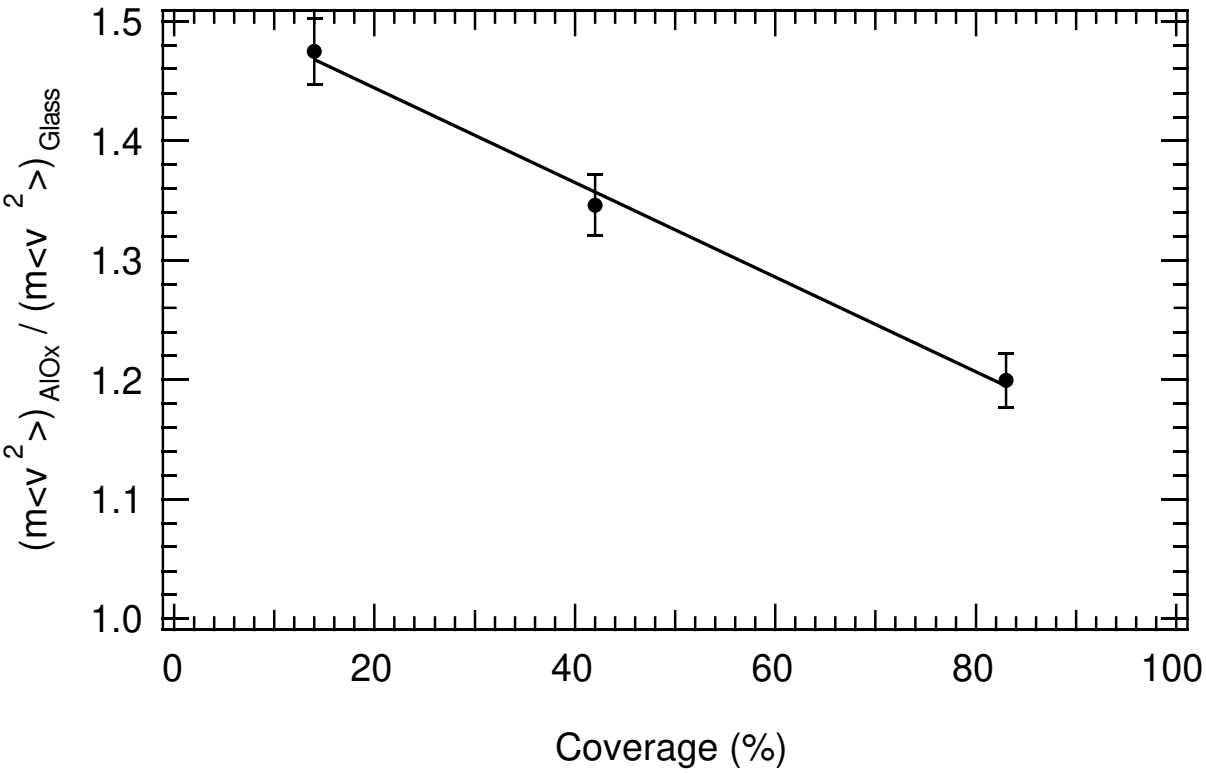

FIG. 4. Ratio of kinetic energies of aluminum oxide and glass particles as a function of coverage. There is no significant dependence on acceleration. The more massive particles have more energy, but the ratio declines as the frequency of interparticle collisions increases.

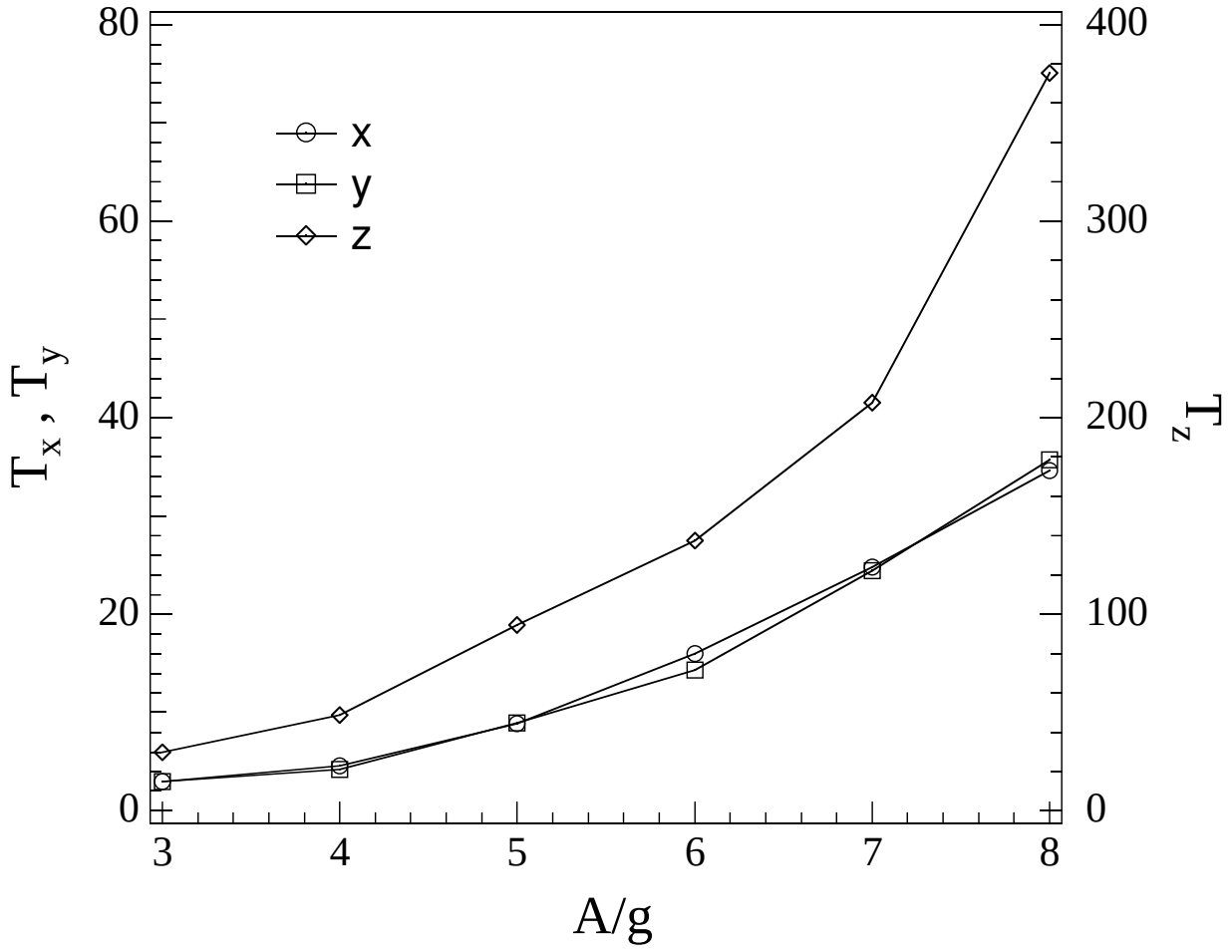

FIG. 5. Variances T_x, T_y, and T_z in the *numerical simulation* as a function of the driving acceleration amplitude A, for 38% coverage and coefficient of restitution $\epsilon = 0.9$. We have used a sampling interval of 0.1 s in the simulations for comparability with the experiments of Fig. 3. Note that $T_x = T_y$ but $T_z > T_x$.

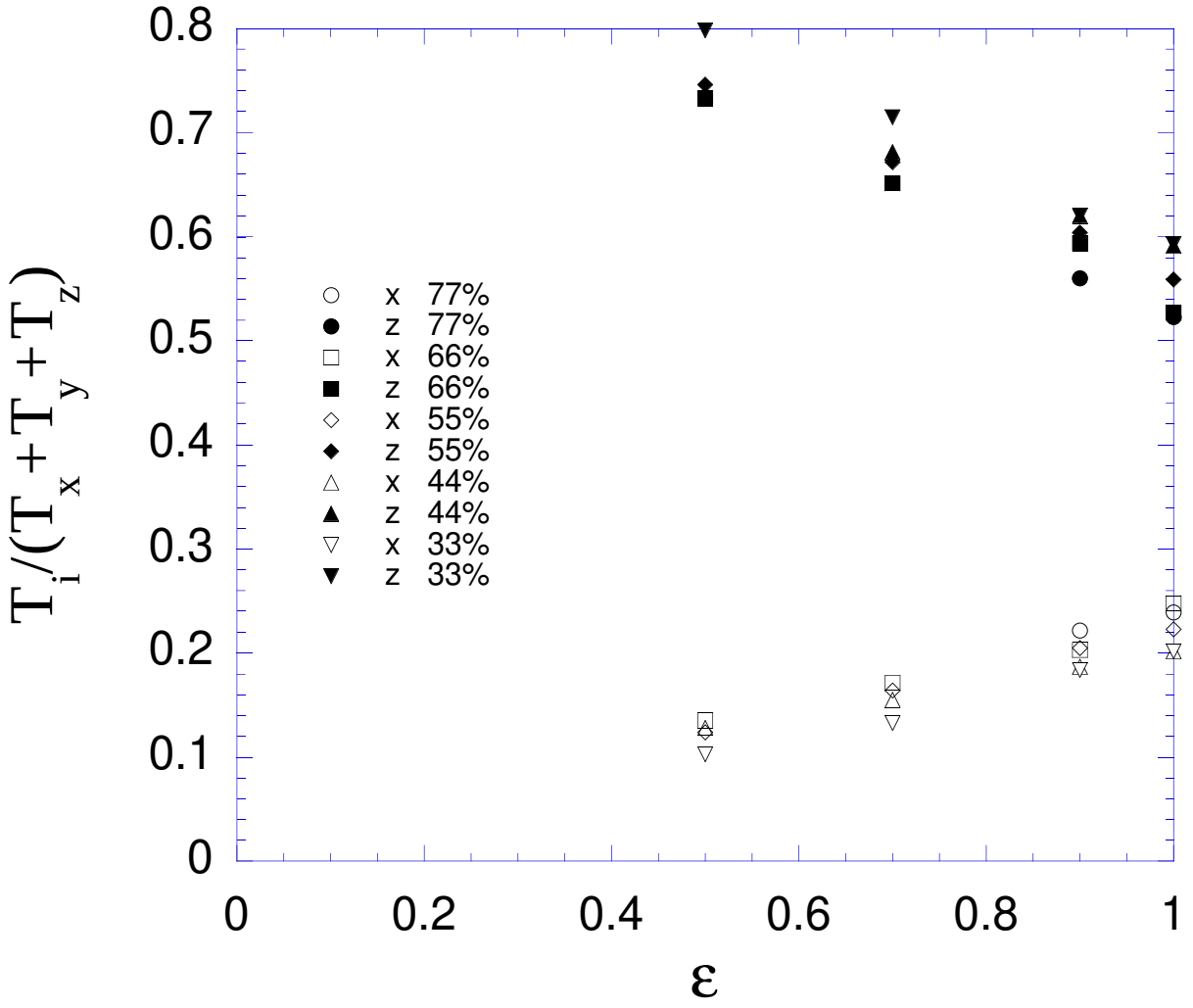

FIG. 6. Fractional kinetic energy corresponding to x, y and z-motions in the *numerical simulation*, for several fractional coverages, as a function of the coefficient of restitution ϵ. Inelasticity augments the anisotropy, but these ratios are independent of coverage.

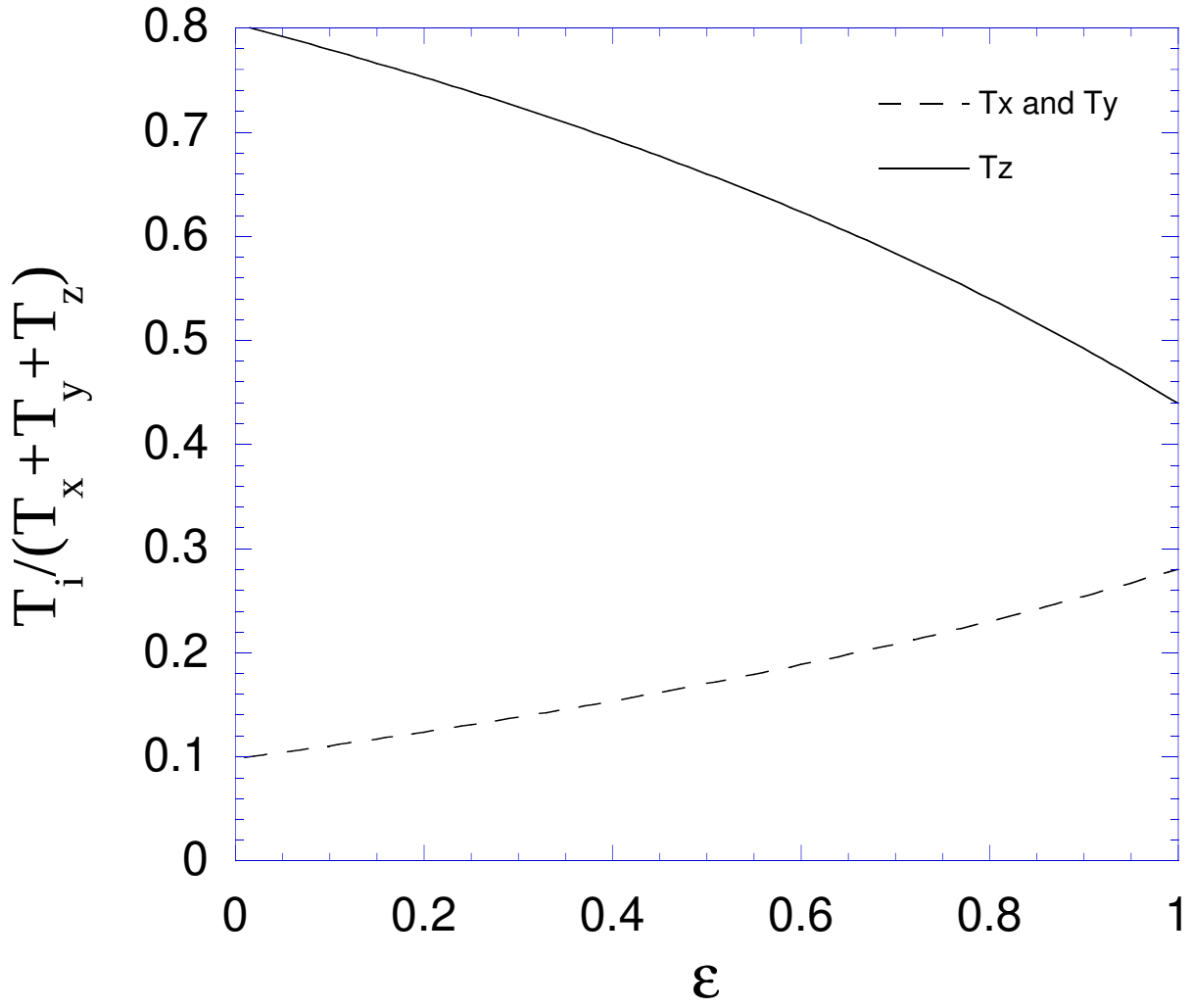

FIG. 7. Fractional kinetic energy corresponding to x, y and z-motions in the *theoretical* prediction of Eq. (1), for several fractional coverages, as a function of the coefficient of restitution ϵ. The behavior is similar to that of the simulation in Fig. 6.

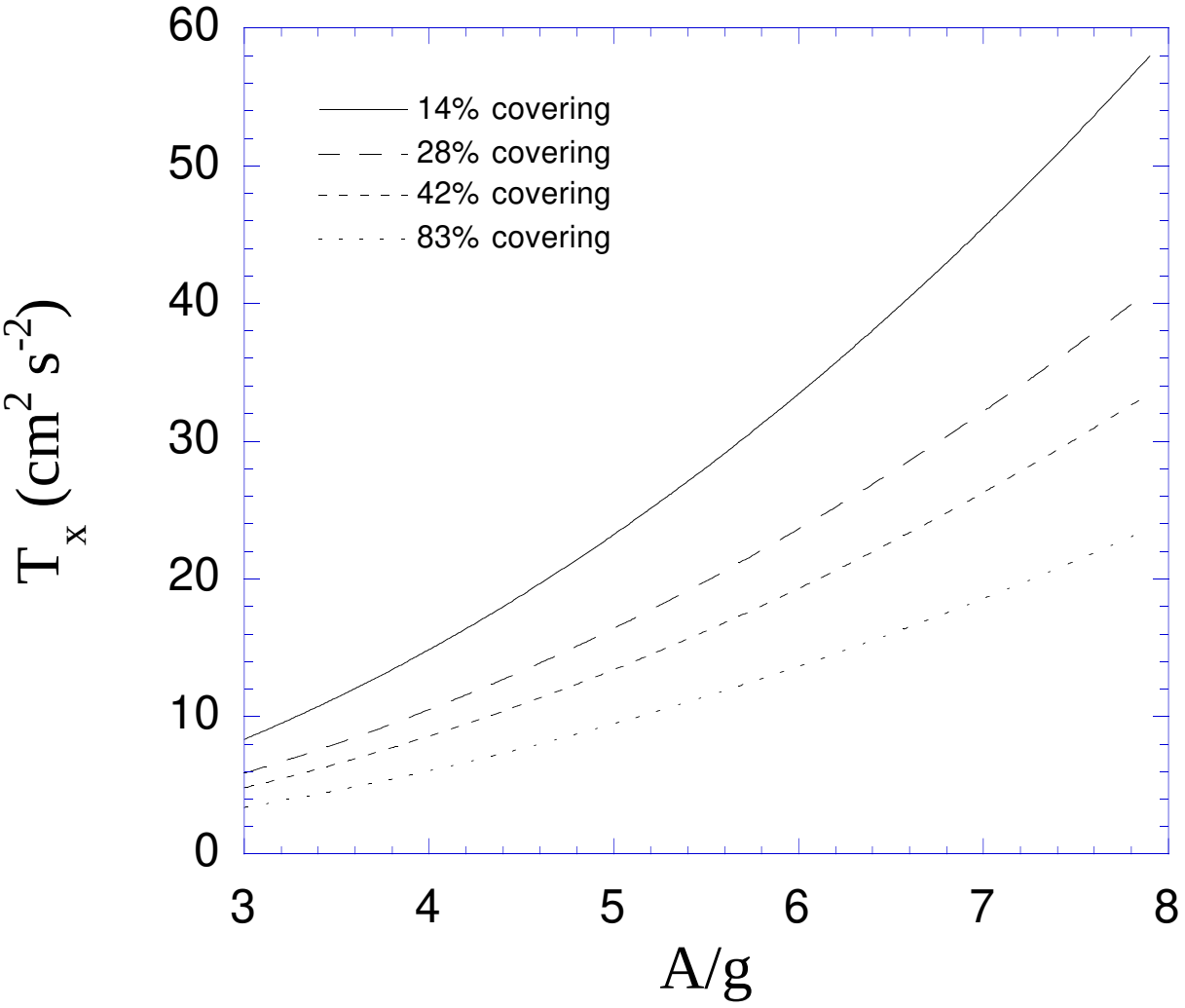

FIG. 8. Theoretical variance T_x of $P(v_x)$ for 4 fractional coverages as a function of acceleration A. It has been reduced by a factor of 2.5 equal to the mean number of collisions in the experimental sampling interval for comparison with the data of Fig.3.